African Journal of Biotechnology Vol. 10(61), pp. 13121-13127, 10 October, 2011
Available online at http://www.academicjournals.org/AJB
DOI: 10.5897/AJB11.538
ISSN 1684–5315 © 2011 Academic Journals

Full Length Research Paper

The effects of gold nanoparticles size and concentration on viscosity, flow activation energy, dielectric and optical properties

Mohamed Anwar K. Abdelhalim[1]*, Mohsen M. Mady[1], Magdy M. Ghannam[1], Mohammed S. Al-Ayed[1] and A. S. Alhomida[2]

[1]Department of Physics and Astronomy, College of Science, King Saud University, Saudi Arabia.
[2]Department of Biochemistry, College of Science, King Saud University, Saudi Arabia.

Accepted 26 August, 2011

This study was carried out to investigate viscosity in relation with the temperature, flow activation energy and dielectric properties for 10, 20 and 50 nm gold nanoparticles size (GNPs) in addition to absorption and fluorescence spectra at different concentrations (0.2×10^{-3} to 1×10^{-2}%) in an attempt to cover and understand the toxicity and potential role of their therapeutic and diagnostic use in medical applications. 10, 20 and 50 nm GNPs dissolved in aqueous solution were purchased (Product MKN-Au, Canada) and used in this study. Mechanical parameters were measured using Brookfield LVDV-III Programmable rheometer with temperature bath controlled by a computer. 0.5 ml of each GNP size in aqueous solution was poured in the sample chamber of the rheometer. The spindle was immersed and rotated in these gold nanofluids in the speed range from 50 to 250 rpm in steps of 20 min. Viscosity of GNPs was measured at temperature of 37°C and at a gradually increase of temperature to 42ºC. UV–Visible characterization of GNPs at different concentrations from 0.2×10^{-3} to 1×10^{-2} % was performed using UV-1601 PC, UV-Visible spectrophotometer. The absorbance measurements were made over the wavelength range of 250 to 700 nm using 1 cm path length quartz cuvettes. Fluorescence characterization of GNPs was performed over the wavelength range of 250 to 700 nm using FluoroMax-2 JOBIAN YVON-SPEX. The measured viscosities for all GNP sizes decreased with increasing the temperatures from 37 to 42°C. The GNPs with larger size (50 nm) exhibited higher viscosity values compared with 10 and 20 nm GNPs. The flow activation energies (kJ/mol) for 10, 20 and 50 nm GNPs were 332.55, 415.4 and 182.2 kJ/mol, respectively. The optical properties such as absorption maxima and the absorption intensity are particle size-dependent. The fluorescence emission band for GNPs with an excitation wavelength of 308 nm and photoluminescence (PL) band centre appeared at 408 nm. With the increase of GNPs concentration at a fixed GNP size of 20 nm, the intensity of emission band positioned increased, and the trend was consistent with the changes of the corresponding surface plasmon resonance (SPR) of GNPs. The presented dielectric data indicates that GNPs have strong dielectric dispersion corresponding to the alpha relaxation region in the frequency range of 20 Hz to 100 kHz which was identified as anomalous frequency dispersion. At a constant GNP size, the absorbance was found to be proportional to the concentration of gold. This is due to the increase in the number of GNPs as well as the increase in the SPR of GNPs. An intense absorption peak was observed at wavelength of 517 nm which is generally attributed to the surface plasmon excitation of the small spherical GNPs. The incident light at 308 nm will lead to excitation of the surface plasmon coherent electronic motion as well as the d electrons. This study suggests that the relaxation of these electronic motions followed by the recombination of the sp electrons with holes in the d band leads to the fluorescence emission. These results indicate that the intensity of fluorescence emission band of GNPs was dependent on the concentration of GNPs. A rapid decrease in the dielectric constant may be attributed to the tendency of dipoles in GNPs to orient themselves in the direction of the applied field in the low-frequency range. However, in the high-frequency range, the dipoles will hardly be able to orient themselves in the direction of the applied field and hence the value of the dielectric constant is nearly constant.

Key words: Gold nanoparticles, viscosity, size, temperature, dielectric, absorption, fluorescence.

INTRODUCTION

Metal nanoparticles (NPs) are attracting a great deal of attention from practitioners in a wide variety of scientific fields (Jana et al., 2001; Schmid, 1994; Schmid et al., I999; Aiken and Finke, 1999; Rao et al., 2000; Templeton et al., 2000; Henglein, 1989; Chen et al., 1998; Jana et al., 1999; Murphy, 2002; Chang et al., 2008). The physical and chemical properties of NPs are directly related to their chemical compositions, sizes, and surface structural characteristics (Wei and Liu, 1999; Mirkin et al., 1996; Taleb et al., 1997; Ascencio et al., 2006); therefore, the design, synthesis, characterization, and applications of nanostructures are critical aspects of the emerging field of nanomaterials.

Among all nanostructured materials, GNPs have attracted particular interest due to their stability, biocompatibility, SPR effect, and unique catalytic activities (Lu et al., 2008).

The recent interest in GNPs is propelled by both the advances in our scientific understanding of their synthesis and physical properties (Daniel and Astruc, 2004; Murphy et al., 2005; Perez-Juste et al., 2005; Alekseeva et al., 2006; Dykman and Bogatyrev, 2007; Jiang and Pileni, 2007; Eustis and El-Sayed, 2006; Jain et al., 2007; Huang et al., 2007) as well as the possibility of using them for the applications in chemical and biological sensing (Daniel and Astruc, 2004; Perez-Juste et al., 2005; Dykman and Bogatyrev, 2007; Huang et al., 2007), cancer treatment (Huang et al., 2007; Huang et al., 2007; Huang et al., 2006; Jain et al., 2007), catalysis (Narayanan et al., 2007), as markers for transmission electron microscopy (TEM) and scanning electron microscopy (SEM) (Horisberger and Rosset, 1977).

Since viscoelastic measurements are nondestructive processes, they can provide information on the structure and elasticity, as well as the storage stability of a material. They can be used for quality control of raw materials, final products, and manufacturing processes. Furthermore, the release of drug from semi-solid carriers is influenced by the rheological behavior as well. The effect of certain parameters such as storage time, and temperature on the quality of pharmaceutical products can also be investigated via rheological measurements.

The origin of the unique optical properties of GNPs is a phenomenon known as SPR. When an electromagnetic radiation of a wavelength much smaller than the diameter of GNPs, hits the particles, it induces coherent, resonant oscillations of the metal electrons across the NPs. These oscillations are known as the SPR, which lie within visible frequencies and result in strong optical absor-bance and scattering properties of the GNPs (Jain et al., 2007).

UV–Vis absorption spectroscopy is the most widely used method for characterizing the optical properties and electronic structure of NPs as the absorption bands are related to the diameter and aspect ratio of metal NPs. At nanometer dimensions, the electron cloud oscillate on the particle surface and absorb electromagnetic radiation at a particular energy. This resonance known as SPR or plasmon absorbance of nanoparticles is a consequence of their small size.

The effects of the nanoparticle size on the rheology properties of GNPs over a temperature range from 37 to 42°C are explored in addition to investigation of the energy loss (ε'') for different GNP sizes in the frequency range of 20 Hz to 100 kHz (at room temperature). Finally, absorption and fluorescence spectra for different GNP sizes dissolved in aqueous solution with different GNP concentrations were investigated.

MATERIALS AND METHODS

Gold nanoparticles (GNPs) size

Different GNP sizes dissolved in aqueous solution were purchased (Product MKN-Au, Canada) and used in this study: the GNPs of size 10 nm (Product MKN-Au-010; concentration 0.01% Au), GNPs of size 20 nm (Product MKN-Au-020; concentration 0.01% Au) and GNPs of size 50 nm (Product MKN-Au-050; concentration 0.01% Au).

Viscosity and flow activation energy measurement

Viscosity

The viscosity of 10, 20 and 50 nm GNPs dissolved in aqueous solution was measured using Brookfield LVDV-III Programmable rheometer (cone-plate viscometer; Brookfield Engineering Laboratory, Incorporation, Middleboro, USA, supplied with temperature bath and controlled by a computer). The rheometer was guaranteed to be accurate within ±1% of the full scale range of the spindle/speed combination in use reproducibility within ±0.2%. The spindle type (SC-40) and its speed combinations will produce results with high accuracy when the applied torque is in the range of 10 to 100%, and accordingly the spindle is chosen.

0.5 ml of each GNP size in aqueous solution was poured in the sample chamber of the rheometer. The spindle was immersed and rotated in these gold nanofluids in the speed range from 50 to 250 rpm in steps of 20 min. The viscous drag of the GNP aqueous solution against the spindle was measured by the deflection of the calibrated spring.

Viscosity of GNPs of different sizes was measured at the started temperature of 37°C and at a gradual increase of temperature to 42°C. Temperature inside the sample chamber was carefully monitored using a temperature sensor during the viscosity measurements.

Flow activation energy

The effect of temperature on the gold nanofluids viscosity was described by the Arrhenius type equation (Mohamed et al., 2000):

$$\eta = \eta_o \varepsilon^{(Ea / RT)}$$

*Corresponding author. E-mail: abdelhalimmak@yahoo.com or mabdulhleem@ksu.edu.sa.

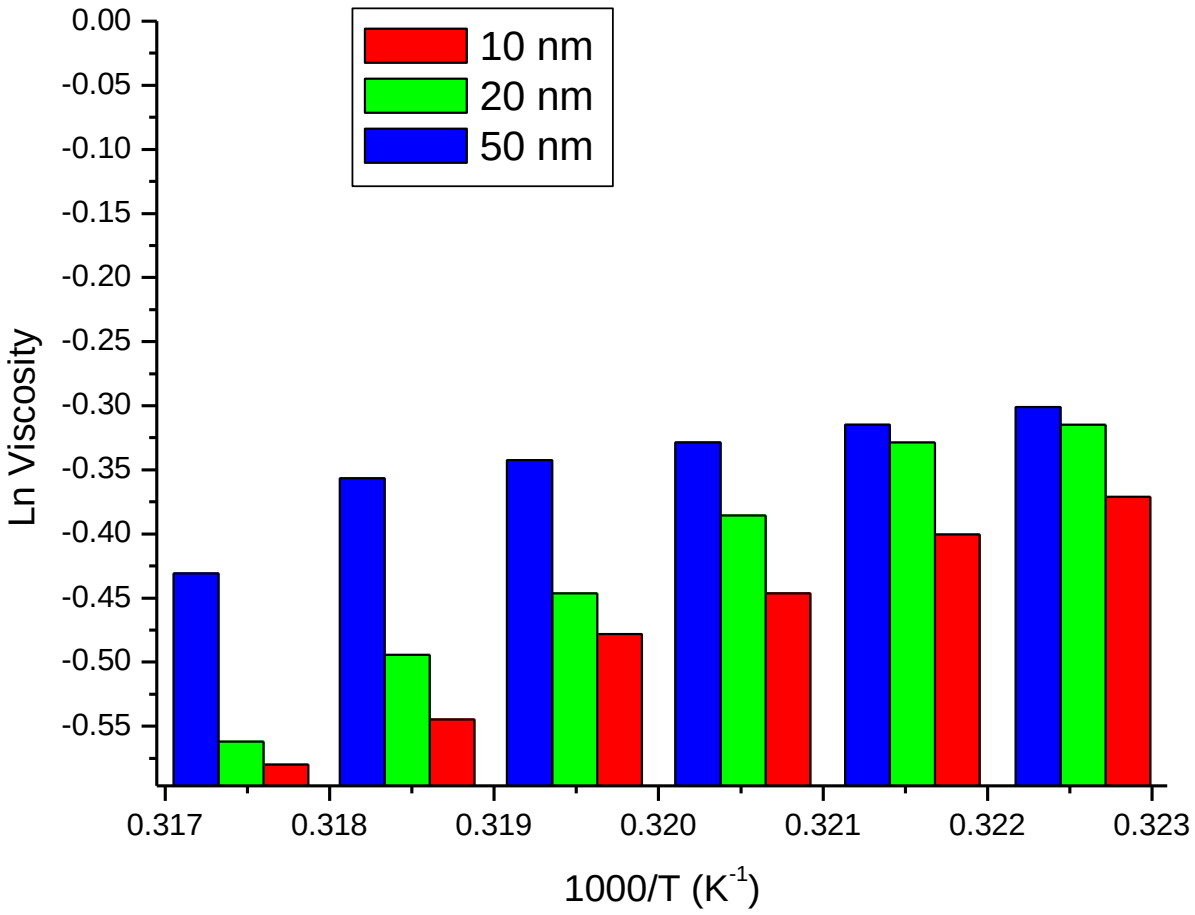

Figure 1. Variation of ln viscosity of GNPs solutions with different sizes.

Where η is the viscosity, η_0 is the viscosity at reference temperature, E_a is the flow activation energy, R is the universal gas constant, and T is the absolute temperature. The E_a for the flow was determined for 10, 20 and 50 nm GNPs.

UV-visible spectroscopy

UV–visible characterization of 10, 20 and 50 nm GNPs dissolved in aqueous solution at different concentrations from 0.2 × 10^{-3} to 1 × 10^{-2}% was performed using UV-1601 PC, UV-visible spectro-photometer, Shimadzu, Japan; H14 granting (UV through shortwave NIR with optical resolution of 0.4 nm). The absorbance measurements were made over the wavelength range of 250 to 700 nm using 1 cm path length quartz cuvettes. The cuvettes were cleaned before each use by sonicating them for 5 min in deionized water and then rinsing with deionized water. The pH value was constant during the measurements for all the examined GNP samples.

Fluorescence spectroscopy

Fluorescence characterization of 10, 20 and 50 nm GNPs was performed using FluoroMax-2 JOBIAN YVON-SPEX, Instruments S.A., Inc., France. The fluorescence measurements were made over the wavelength range of 250 to 700 nm. The fluorescence measurements were made using 1 cm path length quartz cuvettes which were cleaned before each use by sonicating them for 5 min in deionized water and then rinsing with deionized water.

Dielectric parameters

The electrical parameters were measured in the frequency range of 20 Hz up to 1 MHz using a WAYNE KERR precision component analyzer, model 6440 B (UK). The sample cell has two squared platinum black electrodes each having an area of 1 × 1 cm^2 with an inner electrode distance of 1 cm. The measurements were performed at 20°C. For a dielectric material placed between two parallel plate capacitor, the measured values of capacitance (C) and resistance (R) were used to calculate the real (ε') and imaginary part (ε'') of the complex permittivity $\varepsilon^* = \varepsilon' - j\,\varepsilon''$.

RESULTS AND DISCUSSION

Rheology and flow activation energy of GNPs

The measured viscosities for all GNP sizes decreased with increasing GNP temperatures from 37 to 42°C as can be observed in Figure 1. The GNPS with larger size (50 nm) exhibited higher viscosity values compared with

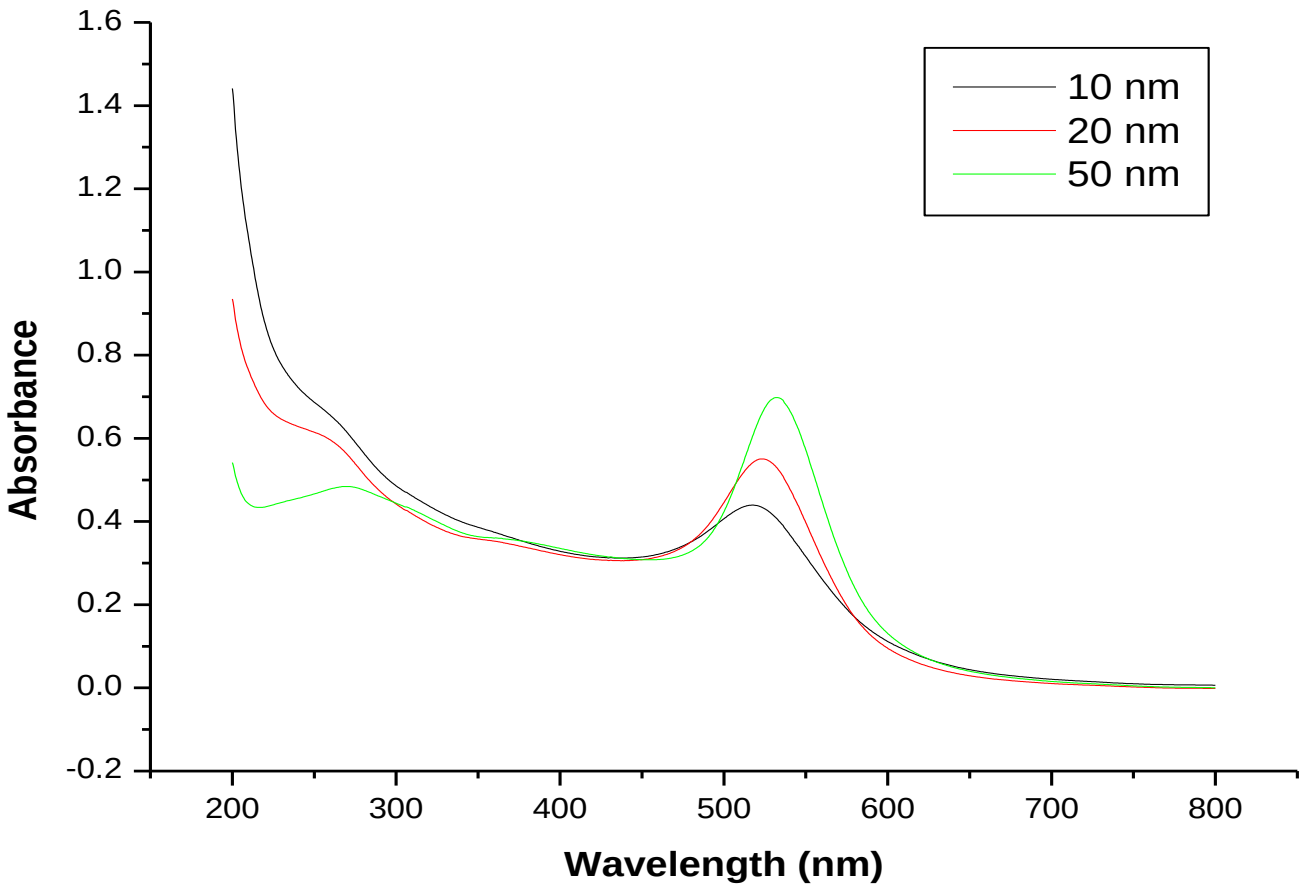

Figure 2. UV-Visible absorption spectra for different GNP sizes at concentration of 0.01%

the 10 and 20 nm GNPs. The evaluated flow activation energies (kJ/mol) for 10, 20 and 50 nm GNPs were 332.55, 415.4 and 182.2 kJ/mol, respectively.

UV-visible spectroscopy

Figure 2 shows the UV–visible absorption spectra for different GNP sizes with the variation of Au absorbance intensity around 517 nm. The optical properties such as absorption maxima and the absorption intensity are particle size-dependent. An intense absorption peak was observed at wavelength of 517 nm which is generally attributed to the surface plasmon excitation of small spherical GNPs.

Figure 3 shows the variation of absorbance of different GNP sizes with the concentration (from 0.2×10^{-3} to 1×10^{-2}%). At a constant GNP size, the absorbance was found to be proportional to the concentration of gold. This is due to the increase in the number of GNPs as well as the increase in the SPR of GNPs.

Single photon luminescence from gold has been described (Lin et al., 2007; Wang et al., 2005) as a three-step process as follows: (i) excitation of electrons from the occupied d to the sp band which is above the Fermi level to generate electron–hole pairs, (ii) scattering of electrons and holes on the picosecond time scale with partial energy transfer to the phonon lattice and (iii) recombination of electron from an occupied sp band with the hole resulting in photon emission.

Fluorescence spectroscopy

The fluorescence emission band for GNPs with an excitation wavelength of 308 nm and the photo-luminescence (PL) band centre appeared at 408 nm as shown in Figure 4. The incident light at 308 nm will lead to excitation of the surface plasmon coherent electronic motion as well as the d electrons. This study suggests that the relaxation of these electronic motions followed by the recombination of the sp electrons with holes in the d band leads to the fluorescence emission which was in agreement with a previous study (Mohamed et al., 2000). With the increase of GNPs concentration at a fixed GNP size of 20 nm, the intensity of emission band positioned was increased, and the trend was consistent with the changes of the corresponding SPB of GNPs as shown in

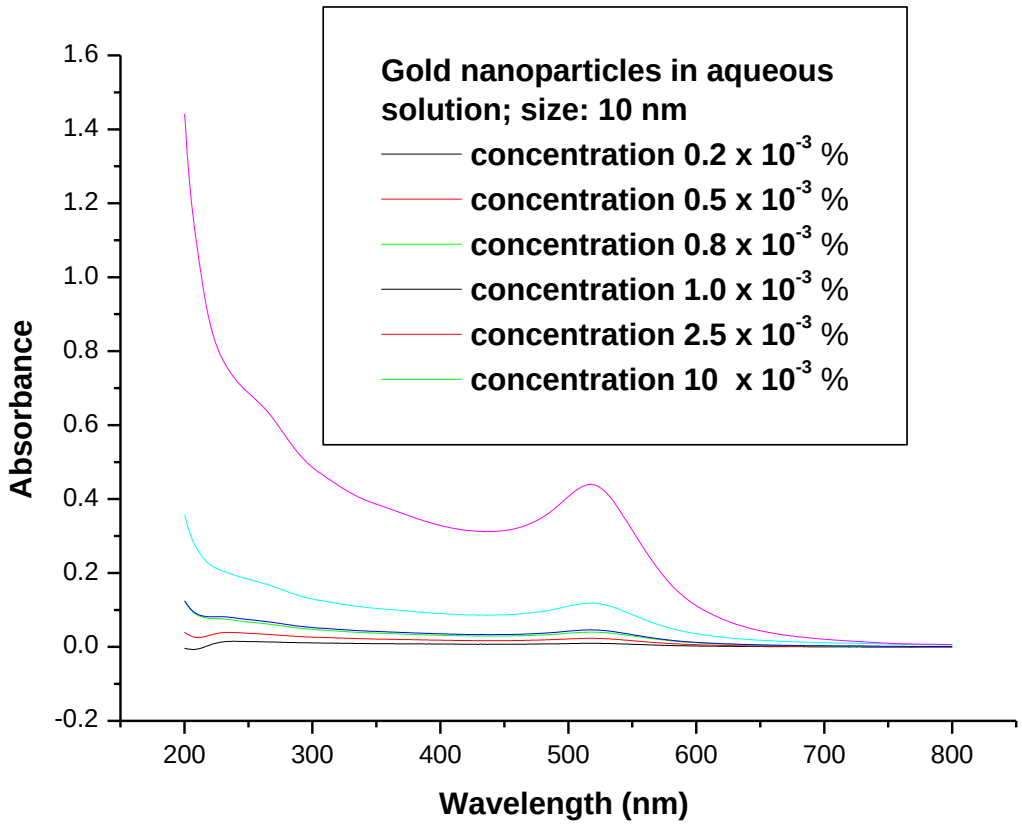

Figure 3. Absorption spectra for GNPs of size 10 nm at different concentrations.

Figure 4. These results indicate that the intensity of fluorescence emission band of GNPs was dependent on the concentration of GNPs.

Dielectric measurements

Figure 5 shows the variation of energy loss (ε'') with the frequency at the room temperature for different GNP sizes (10, 20 and 50 nm). The presented dielectric data indicates that GNPs have strong dielectric dispersion corresponding to the alpha relaxation region in the frequency range of 20 Hz to 100 kHz which identified as anomalous frequency dispersion. A rapid decrease in the dielectric constant may be attributed to the tendency of dipoles in GNPs to orient themselves in the direction of the applied field in the low-frequency range. However, in the high-frequency range, the dipoles will hardly be able to orient themselves in the direction of the applied field and hence the value of the dielectric constant is nearly constant.

Conclusions

The measured viscosities for all GNP sizes decreased with increasing the temperatures from 37 to 42°C. The GNPs with larger size (50 nm) exhibited higher viscosity values compared with the 10 and 20 nm GNPs.

The flow activation energies (kJ/mol) for 10, 20 and 50 nm GNPs were 332.55, 415.4 and 182.2 kJ/mol, respectively.

The absorption maxima and absorption intensity are particle size-dependent. At a constant GNP size, the absorbance was found to be proportional to the concentration of gold. This is due to the increase in the number of GNPs as well as the increase in the surface plasmon resonance of GNPs. An intense absorption peak was observed at wavelength of 517 nm which is generally attributed to the surface plasmon excitation of the small spherical GNPs.

The intensity of fluorescence emission band of GNPs was dependent on the concentration of GNPs. The fluorescence emission band for GNPs with an excitation wavelength of 308 nm and photoluminescence (PL) band centre appeared at 408 nm. With increasing GNPs concentration at a fixed GNP size of 20 nm, the intensity of emission band positioned increased, and the trend was consistent with the changes of the corresponding SPB of GNPs. The incident light at 308 nm will lead to excitation of the surface plasmon coherent electronic motion as well as the d electrons.

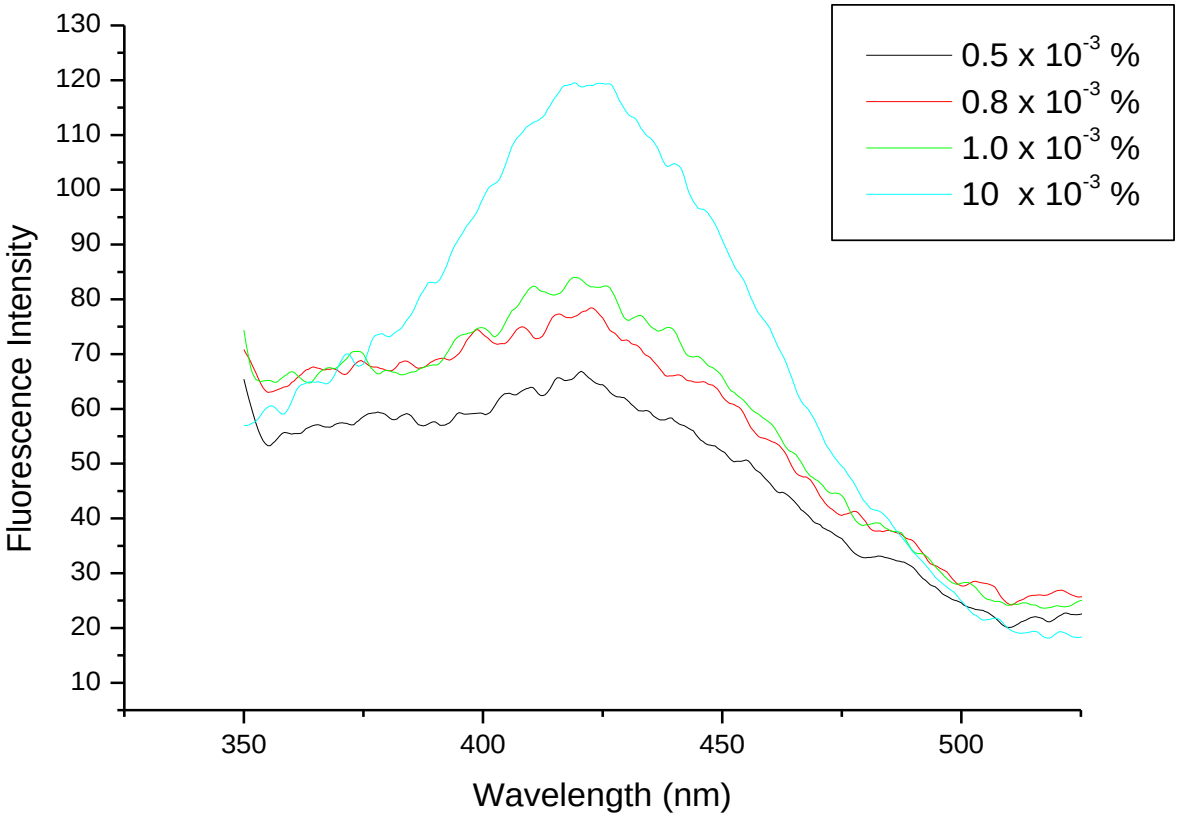

Figure 4. The emission fluorescence band intensity for GNPs of size 20 nm of different concentrations.

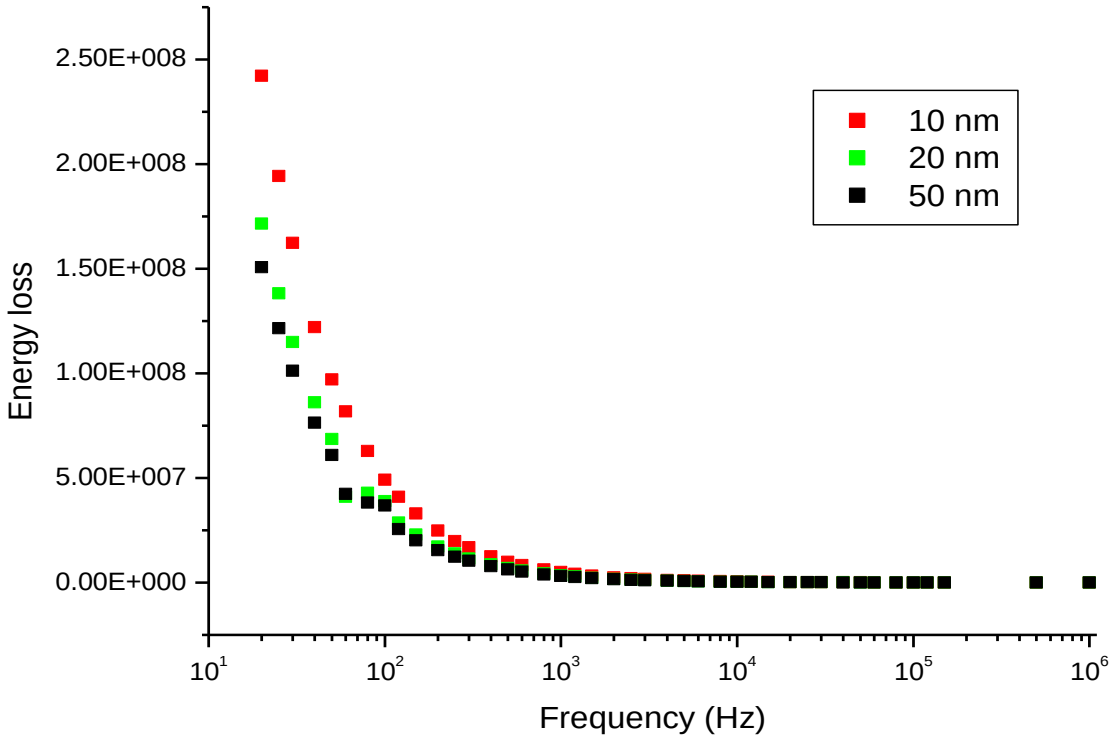

Figure 5. Energy loss ε" as a function of the applied frequency in the range of 20 Hz to 1 MHz for different GNPs (10, 20 and 50 nm).

The GNPs have strong dielectric dispersion corresponding to the alpha relaxation region in the frequency range of 20 Hz to 100 kHz which identified as anomalous frequency dispersion.

ACKNOWLEDGEMENTS

The authors would like to thank Mr. Amgaad for his continuous contribution in the measurements of viscosity, absorption and fluorescence spectra. The authors are very grateful to the National Plan of Science and Technology (NPST). This research was financially supported by the National Plan of Science and Technology Innovation Plan (NSTIP), Research No. 08-ADV206-02 and Research No. 09-NAN670-02, College of Science, King Saud University, Saudi Arabia.

REFERENCES

Aiken JD, Finke RG (1999). Mol. Catal. A-Chem. 145: p. 1.
Alekseeva AV, Bogatyrev VA, Khlebtsov BN, Mel'nikov AG, Dykman LA, Khlebtsov NG (2006Gold nanorods: Synthesis and optical properties. Colloid J. 68: 661-678.
Ascencio JA, Liu HB, Pal U, Medina A, Wang ZL (2006). Transmission electron microscopy and theoretical analysis of AuCu nanoparticles: atomic distribution and dynamic behavior. Microsc. Res. Tech. 69: 522.
Chang TH, Liu FK, Chang YC, Chu TC (2008). Rapidly characterizing the growth of au nanoparticles by CE. Chromatographia. 67: p. 723.
Chen SW, Ingram RS, Hostetler MJ, Pietron JJ, Murray RW, Schaaff TG, Khoury JT, Alvarez MM, Whetten RL (1998). A transition from metal-like double-layer capacitive charging to redox-like charging was observed in electrochemical ensemble Coulomb staircase experiments on solutions of gold. Science, 280: 20-98.
Daniel MC, Astruc D (2004). Gold nanoparticles: assembly, supramolecular chemistry, quantum-size-related properties, and applications toward biology, catalysis, and nanotechnology. Chem. Rev. 104: 293–346.
Dykman LA, Bogatyrev VA (2007). Gold nanoparticles: preparation, functionalisation and applications in biochemistry and immunochemistry. Uspekhi Khimii, 76: 199-213.
Eustis S, El-Sayed MA (2006). Synthesis of metal nanoparticles. Bottom up method--assemble atoms to nanostructures. Chem. Soc. Rev. 35: 209–217.
Henglein A (1989). Small-particle research: Physicochemical properties of extremely small colloidal metal and semiconductor particles. Chem. Rev. 89: 1861-1873.
Horisberger M, Rosset J (1977). Colloidal gold, a useful marker for transmission and scanning electron microscopy. J. Histochem. Cytochem. 25: 295–305.
Huang WY, Qian W, El-Sayed MA, Ding Y, Wang ZL (2007). Atomic structure of Au-Pd bimetallic alloyed nanoparticles. J. Physical Chem 111: 10751–10757.
Huang XH, El-Sayed IH, Qian W, El-Sayed MA (2007). Cancer cell imaging and photothermal therapy in the near-infrared region by using gold nanorods. Nano Lett. 7: 1591–1597.
Huang XH, Jain PK, El-Sayed IH, El-Sayed MA (2007). Gold nanoparticles: Interesting optical properties and recent applications in cancer diagnostic and therapy. Nanomedicine, 2: 681–693.
Huang X, El-sayed IH, Qian W, El-Sayed MA (2006). Cancer cell imaging and photothermal therapy in the near-infrared region by using gold nanorods. J. Am. Chem. Soc. 128: 2115–2120.
Jain P, El-Sayed I, El-Sayed M (2007). Au nanoparticles target cancer. Nano Today, 2: 18–29.
Jain PK, El-Sayed IH, El-Sayed MA (2007). Tthe great potential of laser thermal therapy of cells and tissues conjugated with gold nanoparticles. Nano Today, 2: 18–29.
Jain PK, Huang X, El-Sayed IH, El-Sayad MA (2007). Nanoengineered polymer capsules from fabrication to applications. Plasmonics, 2: 107–118.
Jana NR, Gearheart L, Murphy CJ (2001). Evidence for seed-mediated nucleation in the formation of gold nanoparticles from gold salts. Chem. Mater. 13: 23-13.
Jana NR, Sau TK, Pal T (1999). J. Phys. Chem. B 103: p. 115.
Jiang XC, Pileni MP (2007). Colloids and Surfaces A: Physicochem. Eng. Aspects, 295: 228–232.
Lin A, Son DH, Ahn HH, Song GH, Han WT (2007). Synthesis and spectroscopic characterization of gold nanoparticles. Opt. Exp. 15: p. 6374.
Lu X, Tuan H, Korgel BA, Xia Y (2008). Facile synthesis of gold nanoparticles with narrow size distribution by using AuCl or AuBr as the precursor, Chem. Eur. J. 14: 1584–1591.
Mirkin CA, Letsinger RL, Mucic RC, Storhoff JJ (1996). A DNA-based method for rationally assembling nanoparticles into macroscopic materials. Nature, 382: 607.
Mohamed MB, Volkov V, Link S (2000). The `lightning' gold nanorods: fluorescence enhancement of over a million compared to the gold metal. Chem. Phys. Lett. 317: p. 517.
Murphy CJ (2002). Nanocubes and nanoboxes. Science, 298: 2139.
Murphy CJ, San TK, Gole AM, Orendorff CJ, Gao JX, Gou L, Hunyadi SE, Li T (2005). Anisotropic metal nanoparticles: synthesis, assembly, and optical applications. J. Physical Chem. 109: 13857-13870.
Narayanan R, El-Sayed MA, Chimica OGG (2007). FTIR Study of the Mode of Binding of the Reactants on the Pd Nanoparticle Surface during the Catalysis of the Suzuki Reaction. Chem. Today, 25: 84–86.
Perez-Juste J, Pastoriza-Santos I, Liz-Marzan LM, Mulvaney P (2005). Silica-coating and hydrophobation of CTAB-Stabilized gold nanorods. Coordination Chem. Rev. 249: 1870-1901.
Rao CNR, Kulkarni GU, Thomas PJ, Edwards PP (2000). The size-induced metal-insulator transition in colloidal gold. Chem. Soc. Rev. 29: p. 27.
Schmid G (1994). Clusters and Colloids: From Theory to Applications, VCH, New York.
Schmid G, Baumle M, Geerkens M, Helm I, Osemann C, Sawitowski T (I999). Chem. Soc. Rev. 28: 179.
Steffe J (1996). Rheological methods in food process engineering, 2nd Ed. Freeman Press, Mitchigan State University, USA, p. 21.
Taleb A, Petit C, Pileni MP (1997). Synthesis of highly monodisperse silver nanoparticles from AOT reverse micelles: A way to 2D and 3D self-organization. Chem. Mater. 9: p. 950.
Templeton AC, Wuelfing MP, Murray RW (2000). Monolayer-protected cluster molecules. Acc. Chem. Res. 33: p. 27.
Wang H, Huff TB, Zweifel DA, He W, Low PS, Wei A, Cheng JX (2005). Gold nanorods as contrast agents for biological imaging: optical properties, surface conjugation and photothermal effects. Proc. Natl. Acad. Sci. USA, 102: p. 15752.
Wei GT, Liu FK (1999). J. Chromatogr. 836: 253.